Kinetics of the BrO + HO_2 reaction over the temperature range T = 246 -314 K

Michael K.M. Ward[†] and David M. Rowley[*]

Department of Chemistry, University College London, 20 Gordon Street, London, WC1H 0AJ, UK.

*Corresponding author.

[†] National Physical Laboratory, Hampton Road, Teddington, Middlesex, TW11 0LW, UK.

Abstract

The kinetics of the reaction between gas phase BrO and HO_2 radicals (1) have been studied over the atmospherically relevant temperature range T = 246 – 314 K and at ambient pressure, p = 760 ± 20 Torr, using laser flash photolysis coupled with ultraviolet absorption spectroscopy.

$$BrO + HO_2 \rightarrow HOBr + O_2 \qquad (1)$$

The reaction was initiated by the generation of bromine monoxide radicals following laser photolytic generation of Br atoms from Br_2/Cl_2 containing mixtures and their reaction with ozone. Subsequently, the addition of methanol vapour to the reaction mixture, in the presence of excess oxygen, afforded the efficient simultaneous post-photolysis formation of HO_2 radicals using well-defined chemistry. The decay of BrO radicals, in the presence and absence of HO_2, was interrogated to determine the rate coefficients for the BrO + BrO and the BrO + HO_2 reactions. A detailed sensitivity analysis was performed to ensure that the BrO + HO_2 reaction was unequivocally monitored. The rate coefficient for reaction (1) is described by the Arrhenius expression:

$$k_1\,(T/\mathrm{K}) = (9.28\,^{+7.17}_{-4.04}) \times 10^{-12} e^{\left(\frac{(316 \pm 157)}{T}\right)} \mathrm{cm^3\ molecule^{-1}\ s^{-1}}$$

where statistical errors are 1σ. The negative temperature dependence of this reaction is in general accord with those reported by previous studies of this reaction. However, the present work reports greater absolute values for k_1 than those of several previous studies. An assessment of previous laboratory studies of k_1 is presented. This work confirms that reaction (1) plays a significant role in HOBr formation throughout the atmosphere following both anthropogenic, biogenic and volcanic emissions of brominated species. Reaction (1) therefore contributes to an efficient ozone depleting process in the atmosphere, and further confirms the significance of interactions between two different families of reactive atmospheric trace species.

1. Introduction

Background

Contrary to its halogen counterpart, chlorine, bromine plays a significant role in affecting global ozone abundances across the vertical atmospheric regions of the troposphere and the stratosphere.[1] The enhanced role of atomic bromine compared to chlorine in the lower atmosphere, the troposphere, is particularly significant, and arises principally from the relatively short lifetimes and efficient photochemical degradation of brominated source gases compared to their chlorinated analogues. This is a direct result of the significant visible spectrum absorption cross-sections of brominated species.[2] The sources of atmospheric bromine are partially anthropogenic (typically halons and methyl bromide)[3] but also comprise a significant biogenic component (typically bromoalkanes)[4]. These latter sources are principally oceanic in origin.[5] Bromine may also be liberated from volcanic processes, which can affect local atmospheric acidity, ozone levels and trace gas constituents.[6,7,8] Reactive atmospheric bromine sources also find provenance from heterogeneous processes, such as 'bromine explosion' events observed typically in polar tropospheric regions as a result of the condensed phase oxidation, liberation and subsequent photolysis of gaseous Br_2 from aerosols.[9] Such events, comprising both heterogeneous and subsequently homogeneous gas phase chemical and photolytic processes, can lead to the episodic depletion of tropospheric ozone,[10,11] which have consequent effects on solar UV irradiance but principally on the oxidative capacity of the air. This affects local pollutants but also global species which may act as greenhouse gases, such as methane. Further, bromine is also implicated in the oxidation and reactivity of atmospheric mercury.[12] This has implications for the conversion of gaseous elemental mercury, GEM, into reactive gaseous mercury RGM, which is not only a neurotoxic pollutant, but also acts as an indicator of the extent of mercury pollution in the atmosphere, itself a marker for general anthropogenic pollution. Despite its lower atmospheric abundance than chlorine, bromine also plays a considerable role in the stratosphere, both as a direct ozone depleting substance, but also as an indicator, through coupled bromine - chlorine chemistry, of the extent of chlorine activation and therefore ozone loss.[13,14] The effects of bromine on atmospheric composition are therefore manifold and result

from significant anthropogenic and natural factors, with considerable environmental implications. Understanding bromine chemistry in the atmosphere is consequently of importance. Key reactions involve those of BrO radicals with themselves but also with other trace species, notably peroxy radicals, the understanding of which is the principal objective of this study.

BrO radicals

Photolytic release of bromine atoms from source gases in the atmosphere is typically followed by the formation of bromine oxide radicals, BrO through the reaction of Br with ozone:

$$Br + O_3 \rightarrow BrO + O_2 \qquad (2)$$

Subsequent reactions of BrO to regenerate Br therefore lead to catalytic ozone loss. One such process is the self-reaction of BrO:

$$BrO + BrO \rightarrow Br + Br + O_2 \qquad (3a)$$
$$BrO + BrO \rightarrow Br_2 + O_2 \qquad (3b)$$

This reaction has been extensively studied in the laboratory, as discussed below, and has been directly implicated in episodic ozone depletion events in the polar marine boundary layer, as indicated above.

Bromine oxide radicals may however also interact with other radical families, notably the odd-hydrogen species OH and HO_2 (HO_x). One such process involving reaction (1) provides a further route to potential loss of atmospheric ozone, through the formation and subsequent solar photolysis of HOBr, in a cycle first proposed by Yung *et al.*[15]

$$BrO + HO_2 \rightarrow HOBr + O_2 \qquad (1), (1a)$$
$$BrO + HO_2 \rightarrow HBr + O_3 \qquad (1b)$$
$$HOBr + h\nu \rightarrow OH + Br \qquad (4)$$
$$OH + O_3 \rightarrow HO_2 + O_2 \qquad (5)$$

	$Br + O_3$	$\rightarrow$	$BrO + O_2$	(2)
Net:	$2\,O_3$	$\rightarrow$	$3O_2$	

Taking account of this cycle, and with the inclusion of estimated biogenic sources of atmospheric bromine, as demonstrated by Yang *et al.*[16] yields modelled BrO radical concentrations between 1 – 8 pptv. This is commensurate with a predicted potential interaction of BrO radicals with HO_x species, given previously reported kinetics. This was emphatically demonstrated in a model study by Salawich *et al.*[17], who showed that the extent of upper troposphere odd-oxygen loss is actually dominated by the reaction between BrO and HO_2 radicals below altitudes of *ca.* 15 km.

On account of this importance of bromine oxide – odd hydrogen coupling, several laboratory studies of the BrO + HO_2 reaction have been reported. However, whilst the ambient temperature kinetics of this reaction show some consensus, the temperature dependence of this reaction, as discussed below, is less well-characterised, by a factor of nearly 25% (the JPL - NASA uncertainty factor[2] for k_1 is 1.235 at T = 246 K), examination of which was the principal goal of the present study.

Previous Studies of the BrO + HO_2 reaction

Several previous studies on the kinetics of the BrO + HO_2 reaction have been reported using a variety of techniques including photolytical/spectroscopy and discharge-flow tube/mass spectrometry methods, which are summarised here. The initial study was reported by Cox and Sheppard, applying molecular-modulation UV absorption spectroscopy technique to a $Br_2/O_3/H_2/O_2$ photolysis system at T = 303 K and p = 1 atm.[18] Poulet *et al.* used discharge flow with mass spectrometry to measure k_1 under conditions of excess HO_2 at T = 298K and p = 1 Torr. BrO and HO_2 were generated in this study *via* the microwave produced $O(^3P)$ + Br_2 and Cl + CH_3OH/O_2 reactions respectively.[19] Bridier *et al.* employed the photolysis of $Br_2/O_3/Cl_2/CH_3OH/O_2$/He mixtures at T = 300 K in which HO_2 and BrO radical concentrations, in nearly equal initial abundances, were monitored *via* dual wavelength UV absorption spectroscopy at λ = 210 nm (HO_2) and λ = 313.5 and 329.5 nm (BrO) respectively[20] In a development of the Poulet *et al*. study, and using the same chemical scheme, Larichev *et al.* studied k_1 *via* the discharge flow mass spectrometric method over the temperature range T = 233 – 344 K with an excess of HO_2 over BrO.[21] Elrod *et al.* studied k_1 in a turbulent discharge flow system at a total pressure of p = 130 mbar at T = 298 – 210 K using detection, following titration of radicals, by chemical ionisation mass spectrometry.[22] As with previous discharge flow studies, k_1 was determined by monitoring the BrO radical concentrations in an excess of HO_2 radicals. BrO was produced by the $O(^3P)$ + Br_2 reaction and HO_2 by the H + O_2 + M reaction. Li *et al.* also employed a discharge-flow reactor coupled with molecular beam mass spectrometry to determine k_1 over the temperature range T = 233 – 348 K and p = 1 – 3 Torr. In this case, BrO radicals were produced by the Br + O_3 or $O(^3P)$ + Br_2 reactions and HO_2 radicals were produced by the F + H_2O_2 or Cl + CH_3OH (+ O_2) reactions.[23] Experiments were carried out under conditions of both [BrO] << [HO_2] and [HO_2] << [BrO]. Cronkhite *et al.* studied k_1 at T = 296 K and p = 12 and 25 Torr using laser flash photolysis of $Cl_2/CH_3OH/O_2/Br_2/O_3/N_2$ mixtures with UV absorption spectroscopy at λ = 308 nm, to detect BrO, coupled with simultaneous time-resolved detection of HO_2 at 1372 cm^{-1} by infrared tuneable diode laser absorption spectroscopy.[24] Bedjanian *et al.* studied k_1 using discharge flow between T = 230 and 360 K and at a total pressure of p = 1 Torr of helium.[25] In these experiments BrO radicals were produced by either the Br + O_3 or the $O(^3P)$ + Br_2

reactions and the HO_2 radicals were synthesised by the F + H_2O_2 reaction. Experiments were carried out under conditions of both [BrO] << [HO_2] and [HO_2] << [BrO]. Most recently, Bloss *et al.*[26] studied k_1 at T = 298 K and p = 760 Torr using the technique of flash photolysis/time resolved UV absorption spectroscopy. BrO and HO_2 radicals were generated *via* the Br + O_3 and Cl + CH_3OH/O_2 methods respectively at T = 298 K and p = 760 Torr of O_2.

Evidently, both photolytic techniques employing spectroscopy, or flow tube techniques employing mass spectrometry have contributed considerably to the database for k_1. These techniques do however occupy different chemical and physical regimes, which is discussed further below. A summary of the reported kinetics for reaction (1) is given in Table 1. There remains considerable discrepancy in the reported rate coefficient of reaction (1) under low temperature atmospheric conditions.

Aside from the overall kinetics of reaction (1), the potential branching between channels (1a) and (1b) has also been investigated previously. Neither Bedjanian *et al.*[25] or Larichev *et al.*[21] detected any evidence for ozone formation *via* channel (1b), therefore reporting branching ratios of < 0.015 and < 0.004 from this channel respectively, based upon detection limits. This is supported by theory, from, for example, Guha and Francisco[27] and Kaltsoyannis and Rowley[28]. Both of these studies show that reaction (1) proceeds along a triplet potential energy surface, with a near zero temperature dependence overall, but with a significant barrier to the HBr + O_3 (*ca* 90 kJ mol^{-1}) product channel (1b).

Experimental

Principles of the experiment

The BrO + HO_2 reaction was studied in a manner analogous to those of our recent studies of the ClO + HO_2 and the ClO + CH_3O_2 reactions, which also provide a summary of the apparatus.[29,30] Briefly, initial laser photolytic generation of in this case the bromine oxide radical was accompanied by intervening experiments, with the introduction of hydroperoxy radical precursors, namely chlorine and methanol in the presence of oxygen. Rapid formation of hydroperoxy radicals simultaneous with that of BrO was therefore achieved, and $[HO_2]_0$ was quantified by the depletion in initial $[BrO]_0$. The temporal traces of BrO decay, obtained unequivocally through broadband ultraviolet absorption spectroscopy employing charge coupled device (CCD) detection, showed sensitivity to the kinetics of reaction (1) which were modelled and fitted to determine k_1. The principal reactions are discussed below. Full reaction schemes for the modelling and analysis of the generation and subsequent chemistry of BrO radicals and BrO with HO_2 radicals are given in Tables 2 and 3.

Radical generation

Precursor gases were delivered through Teflon tubing linked to a Pyrex mixing line where they were mixed and diluted in an O_2 or synthetic air (BOC, > 99.98%) carrier gas flow. These were passed to a reaction vessel for laser photolysis and ultraviolet absorption spectroscopy. The flow rates of the non-corrosive N_2 and O_2 gases were set using calibrated mass flow controllers (MKS), whereas the Cl_2 (BOC, 5% by volume in nitrogen, >99% purity) was controlled by a Teflon needle valve with the flow measured by a calibrated glass ball meter. Both bromine and methanol vapours were supplied to the mixing line by passing flow controlled nitrogen through different lines to two separate Pyrex bubblers containing either bromine (Acros, 99.8%) or methanol (Sigma Aldrich, 99.9%) held at T = 0 °C in an ice bath in Dewar vessels. Bromine concentrations were determined spectroscopically *via* UV absorption experiments with Br_2 absent/present in the reactor. Absorbances were fit to the JPL NASA recommended absorption cross-sections[2] using the Beer-Lambert law and good agreement was found

between measured concentrations and those expected from the corresponding vapour pressure and flow rates of bromine at the bubbler temperature. Methanol concentrations were similarly calculated from flow rates and vapour pressure. These concentrations were also confirmed separately *via* gravimetric analysis as previously described by Stone and Rowley.[31] Ozone was generated *in situ* by flowing oxygen through a chamber containing a "pen-ray" mercury lamp, the emitted UV radiation of which photolysed a small amount of the O_2 to facilitate the $O + O_2$ (+ M) reaction. This method of producing O_3 was calibrated at different flows of oxygen, spectroscopically[2] using UV absorption, as with the Br_2 monitoring. The reaction mixture was temperature controlled, to within ± 0.5 K by recycling perfluoroether fluid (Galden HT180) supplied from a thermostat unit (Huber CC180) through a jacket on the reaction vessel.

Initial concentrations of the precursor gases in the reaction mixture were in the ranges $[Br_2] = (0.96 – 2.0) \times 10^{16}$ molecule cm^{-3}; $[Cl_2] = (1.5 – 3.1) \times 10^{16}$ molecule cm^{-3}; $[O_3] = 2.5 \times 10^{15}$ molecule cm^{-3}; $[CH_3OH] = (1.3 – 6.6) \times 10^{17}$ molecule cm^{-3} with a balance concentration of oxygen or synthetic air of *ca.* 2.5×10^{19} molecule cm^{-3}. However, some pre-photolysis chemistry was observed and accounted for as discussed below. The individual flow rates to produce these initial concentrations were calculated to ensure rapid radical formation upon laser photolysis, and a fresh gas mixture for every laser photolysis event.

The radical species BrO and thereafter HO_2 were generated using excimer laser flash photolysis (Lambda-Physik CompEX 201) of precursor gases at $\lambda = 351$ nm. The laser photolysis rate was such that an fresh flow of gases was initialised in each pule, typically 5 seconds per pulse. Initially, the photolysed $Br_2/Cl_2/O_3$ in an O_2 or air carrier flow generated the precursor atoms Br and Cl:

$$Br_2 + h\nu \rightarrow 2\ Br \qquad (6)$$

$$Cl_2 + h\nu \rightarrow 2\ Cl \qquad (7)$$

Subsequently, Br atoms reacted with ozone to generate BrO *via* reaction (2), whilst Cl atoms reacted with Br_2 producing more Br:

$$Cl + Br_2 \rightarrow Br + BrCl \quad (8)$$

which went on to produce further BrO through reaction (2).

Upon the introduction of methanol, the photolysis of the $Br_2/Cl_2/O_3/CH_3OH/N_2$ mixture led to competitive formation of CH_2OH radicals, and, in the presence of excess oxygen, HO_2:

$$Cl + CH_3OH \rightarrow HCl + CH_2OH \quad (9)$$

$$CH_2OH + O_2 \rightarrow HO_2 + HCHO \quad (10)$$

It was essential that precursor concentrations, listed above, were designed to achieve rapid and stoichiometric radical formation, using the well-established rate constants for reactions (2), (8), (9) and (10).[2] Consequently, this design of initial concentrations also had to take into account pre-photolysis precursor equilibration, specifically that between Br_2 and Cl_2 to form BrCl.

$$Br_2 + Cl_2 \rightleftharpoons 2\,BrCl \quad (11)$$

Given the nature of these experiments, the introduction of Cl_2 and therefore the existence of equilibrium (11) meant that the extent of Br radical production upon laser photolysis could not be simply inferred from experiments carried out without chlorine. Analysis of the Br_2/ Cl_2 equilibration (11) was therefore carried out to further establish the pre-photolysis concentrations of BrCl at varying levels of added Cl_2. This arithmetic analysis employed the value of K_{11} = 10.1 ± 0.1 at T = 298 K (the gas mixing line temperature), as reported by Maric *et al.*[32] The analysis of the pre-photolysis concentrations taking account of the equilibration (11) demonstrated that at higher $[Cl_2]$ in the reaction mixture, the ratio of actual pre-photolysis $[Cl_2]/[Br_2]$ to the admitted concentrations, based upon flow rates, was enhanced by up to a factor of 2.3 at the highest levels of chlorine introduced. This had a serendipitous effect of increasing the initial post photolysis concentration of HO_2 and therefore the sensitivity of BrO traces to reaction (1).

Radical Monitoring

BrO radicals were monitored using UV absorption spectroscopy. Light from a xenon arc lamp (Hamamatsu) was collimated and passed through the reaction mixture and focussed into a 0.25 m focal length spectrometer (Chromex) fitted with toroidal mirrors. Spectrally resolved light was then imaged onto the top 31 rows of a 2 dimensional charge coupled device (CCD) array (Wright Instruments). Signal (photocharge) was transferred row by row down the array, out of the illuminated region, to record sequential wavelength and time resolved transmission spectra of the photolysed mixture on kinetic timescales, as shown, specifically for BrO, in our previous studies.[33,34,35] Spectra were recorded over the wavelength range λ = 274 – 338 nm, at a spectral resolution of 1.1. nm full width half maximum. Typically, 1000 sequential spectra were recorded on a timescale of 50 μs/spectrum.

Analysis of radical production routes

Given a knowledge of the precursor halogen concentrations, taking account of the equilibration between Br_2 and Cl_2 and the known absorption cross-sections of Br_2, Cl_2 and BrCl, as shown in Figure 1, the initial post photolysis radical concentrations were also predicted. This was expressed as a factor δ, defined as the ratio of initial $[Cl]_0$ to the total initial radical yield (defined as $[TR]_0$) upon photolysis:

$$[Cl]_0 = \delta \times [TR]_0 \quad \text{(i)}$$

Intuitively,

$$[Br]_0 = (1 - \delta) \times [TR]_0 \quad \text{(ii)}$$

These calculated ratios were examined in a model as a function of the initially admitted $[Cl_2]_0/[Br_2]_0$ ratio, with and without the equilibration of the two halogen species, as shown in comparison with spectroscopic experiments in Figure 2. This demonstrated that Br_2 and Cl_2 do equilibrate pre-photolysis on the timescale of precursor gas mixing in this experiment. This allowed the prediction of initial post-photolysis halogen atom concentrations through the known precursor absorption cross-sections. Subsequently

the maximisation, through kinetic simulations, of the sensitivity of these experiments monitoring BrO to the kinetics of reaction (1) was achieved, as discussed below.

Photolysis experiments were undertaken using several different gas compositions. Absorption spectra for the principal absorbing species involved post photolysis are shown in Figure 3. Time averaged post (relative to pre) photolysis absorbance spectra are presented for four such conditions in Figure 4 (a) - (d). The vibronic absorptions ($A^2\Pi \leftarrow X^2\Pi$) from ClO and BrO are clearly evident in the presence of solely (a) chlorine and (b) bromine respectively. When both halogens are simultaneously introduced, the ClO signal is completely absent (c), since photolytically produced Cl atoms, under the chemical conditions used here, are titrated into Br through their rapid reaction with Br_2 (8). When methanol is introduced to this system, the averaged BrO signal is depleted (d), showing the loss of initially formed Cl atoms to form HO_2, and the subsequent loss of BrO through reaction (1).

Spectral analysis

The time-resolved BrO concentrations, $[BrO]_t$, were obtained by fitting a reference spectrum to each of the sequential experimental spectra using the Beer-Lambert law. This fitting also employed 'differential' spectroscopy whereby an entire BrO spectrum was high pass filtered and fitted to the experimental spectrum. This enabled unequivocal determination of BrO concentrations at each time point, despite the presence of other absorbers, as has been demonstrated in our previous work.[33,34,35]

The BrO reference spectra were taken from the work of Wilmouth *et al*.[36] These cross-sections are reported at higher spectral resolution (0.4 nm FWHM) than spectra recorded in the present study (1.1 nm FWHM), so a smoothing function using a Gaussian averaging kernel, was applied to the reference spectrum. Spectral subtraction gave a minimal residual ($<10^{-4}$ absorbance units) compared to the absolute signal (typically $> 10^{-2}$ absorbance units) in the fitting procedure.

Subtraction of the BrO signal, from fitting as discussed above, showed the clear negative residual absorbance signal (post *vs* pre photolysis) attributed to ozone loss at short wavelengths (λ = <320 nm). Figure 5 illustrates this, comparing the residual experimental absorbance over λ = 274 – 317 nm to that of the literature ozone cross-section, and their clear negative correlation.

Data analysis and results

BrO in the absence of HO_2 precursors: the BrO self-reaction

In these experiments, both Br_2 and Cl_2 were photolysed in the presence of ozone. As shown in Figure 4(c), this led to the exclusive formation of BrO radicals following reactions (2), (6), (7), and (8). Both $[BrO]_t$ and the (change in) ozone concentration $[\Delta O_3]_t$ were temporally monitored pre and post photolysis. An example kinetic trace is shown in Figure 6. This kinetic behaviour is entirely commensurate with the BrO self-reaction and the catalytic loss of ozone. Accordingly, a full reaction system, as presented in Table 2, was used to model and fit to these data, also as shown in Figure 6, and kinetic parameters for the BrO self-reaction were obtained. This dual monitoring enabled both the terminating and non-terminating channel rate coefficients for the BrO self reaction, (3a) and (3b), to be determined. These data are shown in Table 4 and presented graphically in Figure 7. The Arrhenius expressions obtained from these data were:

$$k_{(3a)}(T/K) = 2.47^{+1.71}_{-1.01} \times 10^{-12} e^{\left(\frac{(51 \pm 144)}{T}\right)} \text{cm}^3\text{molecule}^{-1}\text{s}^{-1}$$

$$k_{(3b)}(T/K) = 1.48^{+0.55}_{-0.40} \times 10^{-13} e^{\left(\frac{(624 \pm 87)}{T}\right)} \text{cm}^3\text{molecule}^{-1}\text{s}^{-1}$$

$$k_{(3)}(T/K) = 1.81^{+0.68}_{-0.50} \times 10^{-12} e^{\left(\frac{(247 \pm 88)}{T}\right)} \text{cm}^3\text{molecule}^{-1}\text{s}^{-1}$$

Where errors are 1σ, statistical only. These BrO self-reaction data were used in the subsequent analysis of the BrO + HO_2 reaction.

BrO in the presence of HO_2 precursors: the BrO + HO_2 reaction

Experiments invoking the addition of HO_2 precursors led to a reduction in the initial post photolysis [BrO] (Figure (4d)) and a more rapid loss of BrO, discussed below. Further, the loss of ozone in these experiments was reduced which implied a reduction in the BrO self-reaction to a terminating channel involving BrO, attributed to reaction (1). The total loss of ozone measured in these experiments could thus be simply expressed by consideration of the initial kinetic competition for Cl atoms between bromine or methanol and modelling. Given this, it can be shown that:

$$\frac{1}{\Delta[O_3]} = -\frac{k_8[Br_2]}{k_9[Cl]_0[CH_3OH]} + \frac{1}{[Br]_0} \qquad \text{(iii)}$$

A plot of $(1/\Delta[O_3])$ *vs* reciprocal methanol concentration compared to observations is shown in Figure 8, confirming that such a competition for initially formed halogen atoms exists, leading to a terminating reaction for BrO with HO_2

The $[BrO]_t$ and $\Delta[O_3]_t$ traces were fit to a kinetic model as given in Table 2, but with the additional reactions, notably (1), correlating the two radical families, as presented in Table 3. Typical concentration traces and fits are given in Figure 9. The optimised parameter was k_1, using the values for total initial radical concentration $[TR]_0$ and the partitioning factor δ from alternate experiments without methanol as described above. The kinetic data obtained for reaction (1) are presented in Table 5. These data are presented in Arrhenius form in Figure 10.

The temperature dependence for reaction (1) is described by the Arrhenius expression:

$$k_{(1)}(T/K) = 9.28^{+7.17}_{-4.04} \times 10^{-12} e^{\left(\frac{(316 \pm 157)}{T}\right)} \text{cm}^3 \text{ molecule}^{-1} \text{ s}^{-1}$$

This may be compared to the current IUPAC[37] and NASA[2] ref recommendations of

$$k_{(1)}(T/K) = 4.5 \times 10^{-12} e^{\left(\frac{(500 \pm 200)}{T}\right)} \text{cm}^3 \text{molecule}^{-1} \text{s}^{-1} \qquad \text{(IUPAC)}$$

$$k_{(1)}(T/K) = 4.5 \times 10^{-12}\ e^{\left(\frac{(460)}{T}\right)} \text{cm}^3\text{molecule}^{-1}\text{s}^{-1} \qquad \text{(JPL)}$$

Sensitivity analysis

The BrO self-reaction (3)

The sensitivity of the rate coefficients derived for reaction (3) with respect to the uncertainty in secondary chemistry were minimal, owing to the constraint provided in the fitting procedure *via* the simultaneous monitoring of both $[BrO]_t$ and $\Delta[O_3]_t$ traces. This sensitivity analysis was carried out by taking an optimised pair of $[BrO]_t$ and $\Delta[O_3]_t$ traces generated using the numerical model based upon reactions in Table 2, at T = 298 K and at T = 246 K, then re-optimising the parameters, total radicals $[TR]_0$, k_{3a} and k_{3b} using the same model at the relevant temperature and noting the deviation with perturbation to the model. This process was carried out by halving or doubling each reaction rate coefficient in the mechanism in an iterative manner. The percentage difference between the initial and output (optimised) parameters was then expressed. The results showed that the model, and hence the returned kinetic results, were most sensitive to the rate coefficients for the BrO self-reaction (3a, 3b), as designed. Most other reactions showed insignificant sensitivity. However, at T = 298 K, the effect of perturbing the rate coefficient of the Br + O_3 reaction (2) on k_{3a} and k_{3b} was ± 8%. The effect of perturbing the Cl + Br_2 reaction rate coefficient (8) was more significant: + 20% on doubling k_8, and – 37% on halving k_8. Interestingly, the branching ratio was unperturbed by changing rate coefficients for (2) and (8), indicating that the principal sensitivity lay in the initial radical concentrations generated post photolysis. At T = 246 K, sensitivities were very similar, aside from an increase in the effects of doubling k_2 of + 48%, reflecting the negative temperature dependence of this reaction. It should be noted that these perturbations of the input parameter k_2 by a factor of 2 lie well outside of the JPL NASA recommended uncertainties and are therefore upper limits. At T = 298 K, the recommended uncertainty in k_2 is a factor of 1.15, rising to 1.23 at T = 246 K. In similar fashion, the values of k_{3a} and k_{3b} were reanalysed by perturbing absorption cross-sections for BrO. In this case, the reported uncertainty of ± 11%, as reported by Wilmouth *et al.*[36] for BrO cross-sections was adopted. This led to a near identical perturbation in k_3, as expected from simple kinetic analysis. Overall, we therefore calculate an additional potential systematic uncertainty of 19% in k_3 at T = 298 K, rising to 27% at T = 246 K.

The BrO + HO_2 reaction (1)

An analogous sensitivity analysis was carried out on a corresponding $[BrO]_t$ and $\Delta[O_3]_t$ trace pair using the expanded BrO + HO_2 model (Tables 2 and 3) at T = 298 K and T = 246 K. The results are shown in Figures 11(a) and 11(b), respectively presented as percentage differences for k_1 obtained after reanalysing a characteristic dataset with perturbed input parameters by a multiplicative or divisive factor of 2. Only the principally sensitive reactions (those resulting in $>$ 5% deviation in returned values of k_1) are shown. In similar fashion, sensitivity to initial concentrations of precursor gases was considered. Here, the principal factor was the methanol concentration, which, if halved in the model led to a 25% increase in the returned value of k_1. By contrast, changing the O_3 concentration analogously led to changes in k_1 of within 7%. Finally, perturbation of the BrO absorption cross-sections was investigated, analogous as in the study of reaction (3). Here, the sensitivity parameters were near identical to the reported factor of 1.11 uncertainty in σ_{BrO}. Such an extensive sensitivity analysis was necessary to ensure that the radical formation routes were well characterised and that the flux through the BrO + HO_2 reaction had been maximised. The kinetic uncertainty factors, as with the study of reaction (3), were somewhat greater than those actually recommended by JPL NASA[2] and IUPAC.[37] Thus, these parameters were subsequently scaled down according to the reported uncertainty parameters and combined in quadrature with uncertainties in other parameters discussed above. This led to an overall additional potential systematic error in k_1 of 21% at T = 298 K, rising to 41% at T = 246 K.

Discussion

Comparison with previous studies

The BrO + BrO reaction (3)

Both channels of the BrO self-reaction have recently been studied extensively using the current apparatus as a function of temperature. [34,34,35] The experimental conditions chosen for the present study were similar, the only difference being the use of Cl_2 in the present work as an extra source of Br atoms *via* the reaction of Cl with Br_2 (8). Therefore the results of the current work are compared to the more comprehensive and extensive study of Ferracci *et al.*[33] Figure 7(a) shows that the overall rate constant at $T = 298$ K obtained for reaction (3) is in reasonable, but not statistical, agreement with that reported by Ferracci *et al.* (k_3 (this work) = $4.18 \pm 0.56 \times 10^{-12}$ molecule cm^3s^{-1}, versus (k_3 (Ferracci *et al.*) = $3.39 \pm 0.08 \times 10^{-12}$ molecule cm^3s^-1). Errors at 1 σ. Figure 7(b) shows a near perfect agreement for k_{3a} with the study of Ferracci *et al at* $T = 298$ K., (k_{3a} (this work) = $2.86 \pm 0.10 \times 10^{-12}$ molecule cm^3s^{-1}, versus (k_{3a} (Ferracci *et al.*) = $2.81 \pm 0.09 \times 10^{-12}$ molecule cm^3s-1). but slightly greater values for k_{3b} in this work than previously reported, hence a decreased branching ratio towards reaction (3a) than previously reported from this laboratory, albeit one well within the current JPL NASA reported uncertainty for this reaction. Importantly, the use of k_3 as obtained in this work did not perturb however determinations of k_1, as evidenced by the sensitivity analyses discussed above. Further, k_3 was near identical in experiments conducted before and directly after the intervention of HO_2 precursors.

The BrO + HO_2 Reaction (1)

The ambient ($T = 298$ K) temperature values of k_1 derived in this work and other kinetic studies of reaction are shown in Figure 12. There is a clear divide between studies that agree on a value of k_1 around 2×10^{-11} cm^3 $molecule^{-1}$ s^{-1} and those closer to 3×10^{-11} cm^3 $molecule^{-1}$ s^{-1}. This work reports values in between the two but is closest in agreement with the values reported by Bedjanian *et al.*[25] However, when considering the reported uncertainties of the literature data above, this work also agrees with those of Bloss *et al.*,[26] Bridier *et al.*[20]and Larichev *et al.*[21] The work of Bridier *et al.* and Bloss *et al*. used the flash

photolysis technique and similar reaction schemes at the same pressure as employed in this work. As in the present study, Bloss *et al*. used broadband UV spectroscopy and monitored BrO only whereas Bridier *et al.* used single wavelength spectroscopy to measure both absorption signals from HO_2 and BrO at λ = 210/220 nm and λ = 313/329 nm respectively. As discussed above, there is significant overlap of HO_2 absorption at these wavelengths by other precursor absorbers (principally O_3), therefore the potential for significant uncertainty in the derived [HO_2] is high, perhaps explaining the large error in the Bridier *et al.* value. The main difference between the Bloss *et al*. study and the current one is in the determination of the initial radical number density post-photolysis *i.e.* the actinic calibration and the subsequent treatment of $[Cl]_0/[Br]_0$ resulting from the possible formation of BrCl in the pre-photolysis mixture. Changes in total initial radical concentrations by mixing chlorine and bromine compared to single halogen mixtures do not apply in the present work as identical halogen mixtures were used in the presence and absence of the HO_2 precursor. The measurement of the changes in ozone concentration throughout the entire duration of each photolysis experiment was also made in this work which enabled the determination of the partitioning of $[Cl]_0/[Br]_0$ and any perturbations resulting from equilibrium (11) and subsequent BrCl photolysis. This work implies that there is significant BrCl formation during the transit of the halogen precursors through the mixing line and reactor. This differs from that of Bloss *et al*. who considered the changes in the optical density resulting from the possible formation of BrCl but only as far as to allow their kinetic model to optimise $[Cl]_0$ to account for the discrepancies in the actinic calibration of $[Cl]_0$.

The effect of methanol on the HO_2 self-reaction and how this is accounted for also has a potential impact on the experimentally retrieved rate constants for reaction (1). While the parameterisation of the methanol enhancement on this reaction from Bloss *et al*. would have been suitable in this study at T = 298 K the subsequent Stone and Rowley[31] parameterisation of the methanol enhancement was applied which was within 20% of the Bloss *et al.* values. However, the overall effect on the values of k_1 arising from these differences in approach appears to be small as indicated by their general agreement and the sensitivity parameters discussed above.

All the other studies of BrO + HO_2 were carried out at low pressures and, apart from Cronkite *et al*.,[24] used the discharge flow-tube method. Cronkhite *et al*. used a similar radical

formation chemical mechanism as used in the current work but photolysed Cl_2 and O_3 at λ = 308 nm to generate radicals. BrO was monitored by UV spectroscopy whereas HO_2 was monitored using a tuneable diode laser in the infrared region thus eliminating the problem of overlapping absorbers in the UV as would have been encountered in the Bridier *et al.* work. The principal uncertainty arose in the Cronkhite study from the accuracy in the infrared line strengths to determine [HO_2] which was in excess of [BrO].

The remaining studies discussed below all measured the temperature dependence of reaction (1). For clarity, only the parameterisations of the kinetics of previous studies are shown with the experimental data from this work in Figure 13. This confirms the negative temperature dependence of the BrO + HO_2 reaction.

The determination of k_1 as a function of temperature was first carried out by Larichev *et al.*[21] However it is superseded by the study of Bedjanian *et al.*[25] whose studies were conducted in the same laboratory. Problems concerning the Larichev *et al.* study principally arose through heterogeneous secondary chemistry effects which at the lowest temperature study led to a spurious measurement of k_1. Wall loses are an endemic problematic feature of all flow-tube studies, especially at low temperatures. However, the work of Bedjanian *et al.* employed a different experimental configuration to Larichev *et al.,* aimed at minimising these first order wall losses by changing the HO_2 radical source and moving it into an inner movable injector. Aside from Bedjanian *et al.* who utilised the F + H_2O_2 precursor reaction for HO_2 only, the other studies used the Cl + CH_3OH (+O_2) method of forming HO_2 which also has significant complications arising at low temperatures arising from the potential complexation of HO_2 and CH_3OH. However, Elrod *et al*.[22] used a heated coil to keep the inner movable injector at room temperature whilst Li *et al*.[23] used both methods with both [BrO] in excess of [HO_2] and *vice versa*. Therefore the differences between the low pressure ambient temperature values of k_1 and the high pressure values are difficult to reconcile, but do not indicate a pressure dependence to reaction (1). Bedjanian *et al.* also utilised a relative rate method to determine k_1 which was in excellent agreement with their absolute determinations. The current work reports values in good agreement with the work of Bedjanian *et al.* as shown in Figure 12. Therefore, the experiments in the present work, operated under different conditions to all previous temperature dependence studies aside from temperature, lends

support to a larger room temperature value of k_1 but a slightly weaker temperature dependence than that previously reported.

This is in accordance with computational studies also supporting an apparent lack of pressure dependence for reaction (1) when comparing this work to the previous low pressure studies. Further, the branching ratios inferred from the loss of ozone imply that reaction (1) proceeds principally through channel (1a) at all temperatures.

Conclusions

Reaction (1) has been shown to exhibit kinetically a clear but subtle negative temperature dependence, in keeping with all previous work albeit reporting different absolute values for k_1 from previous studies. Here, the simultaneous monitoring of [BrO] and $\Delta[O_3]$ presented evidence that channel (1a) is completely dominant, in accord with previous experimental and theoretical work. The comparison with this and other atmospheric pressure studies of k_1 with those carried out at low pressures implies a minimal pressure dependence for this reaction. It is clear that reaction (1) may therefore play a key role in both tropospheric and stratospheric ozone loss processes, as already illustrated through model studies.[4] The rate constant we report is:

$$k_{(1)}\,(T/K) = 9.28\,^{+7.17}_{-4.04} \times 10^{-12} e^{\left(\frac{(316 \pm 157)}{T}\right)} \text{cm}^3 \text{ molecule}^{-1} \text{ s}^{-1}$$

Acknowledgements

MW thanks the UK EPSRC for funding a PhD studentship. DMR thanks NERC for research support. Both authors would like to dedicate this work, as with our previous papers on these halogen systems to the memory of Professor Roland von Glasow.

Figure Captions

Figure 1: Absorption cross-sections of, Cl_2 (green), BrCl (blue) and Br_2 (red).[2]

Figure 2**:** Dependence of the function delta (see text for details) against the initial (introduced) halogen concentration. The blue line assumes no pre-photolysis reaction between Cl_2 and Br_2. The black line assumes equilibration of Cl_2 and Br_2 has occurred. Red squares are data inferred from spectroscopic fits.

Figure 3: Absorption cross-sections of BrO (violet), ClO (light blue), HO_2 (green), HOBr (dark blue) and O_3 (red).[2]

Figure 4: Time averaged post photolysis (relative to pre-photolysis) absorption spectra taken over 250 μs post laser photolysis of: (a) Cl_2/O_3/air; (b) Br_2/O_3/air; (c) $Cl_2/Br_2/O_3$/ air; (d) $Cl_2/Br_2/O_3/CH_3OH$/air.

Figure 5: (a) Experimental residual absorbance of post photolysis spectrum after subtraction of halogen oxide radical absorbance contribution (black) and an ozone reference spectrum (blue). (b) Correlation of absorbance (black points) and scaled ozone cross-section (red line). The correlation coefficient (R^2) is 0.998.

Figure 6: Temporal evolution of BrO radicals and ozone following laser photolysis of a bromine ozone mixture. Black points = $[BrO]_t$, blue points = $\Delta[O_3]_t$. Solid lines are kinetic fits to the data, minimising the sum of squares between modelled and measured [BrO]. Laser photolysis is at *ca.* 0.015 s.

Figure 7: Arrhenius plots for BrO dimerization kinetics (reaction (3)). (a) Total rate constant k_3 (squares) compared to the parameterisation of Ferracci *et al.* , solid line; (b) Individual k_{3a} (black squares) and k_{3b} (red squares) compared to the parameterisation of Ferracci *et al.*[33], solid lines. Dotted lines indicate the error bounds from Ferracci *et al.*

Figure 8: Plot of reciprocal ozone change versus reciprocal methanol introduction, with a fit, minimising the residuals according to expression (iii).

Figure 9: A typical (single experiment) plot of $[BrO]_t$ and $\Delta[O_3]_t$ recorded from the photolysis of $Br_2/Cl_2/CH_3OH$/air mixtures at T = 298 K. Several (>50) such experiments were recorded and averaged for the final analysis. Laser photolysis is at *ca.* 0.015 s.

Figure 10: Arrhenius plot for the BrO + HO_2 reaction (1) (points) from the current work, with a least squares parameterisation (line).

Figure 11: Ambient temperature (T = 298 K) determinations of k_1. (a) Bridier *et al.*[20], (b) Larichev *et al.*[21], (c) Elrod *et al.*[22], (d) Li *et al.*[23] (HO_2 in excess) (e) Li *et al.* (BrO in excess)[23], (f) Cronkhite *et al.*[24], (g) Bedjanian *et al.*[25], (h) Bloss *et al.*[26], (i) This work, (j) IUPAC[37] and (k) NASA JPL.[2]

Figure 12: Comparison of Arrhenius plots for k_1, with parameterisation of previous studies. Larichev *et al. .*[21] (red), Elrod *et al.*[22] (orange), Li *et al.* [23], (green) and Bedjanian *et al. .*[25] (blue).

Tables

Table 1: A summary of previous kinetic studies of the BrO + HO_2 reaction (1).

Study	T / K	k_1/ cm^3 molecule^{-1} s^{-1}
Cox and Sheppard18	303	$(0.5\ ^{+0.5}_{-0.3}) \times 10^{-11}$
Poulet *et al.*[19]	298	$(3.3 \pm 0.5) \times 10^{-11}$[a]
Bridier *et al.*[20]	300	$(3.4 \pm 1.0) \times 10^{-11}$
Larichev *et al.*[21]	303	$(3.4 \pm 0.6) \times 10^{-11}$[a]
	233 – 344	$4.77 \times 10^{-12} \exp[(580 \pm 100)/T]$
Elrod *et al.* [22]	298	$(1.4 \pm 0.3) \times 10^{-11}$[a]
	210 – 298	$2.5 \times 10^{-12} \exp[(520 \pm 80)/T]$
Li *et al.* [23]	298	$(1.73 \pm 0.61) \times 10^{-11}$[a]
	298	$(2.05 \pm 0.64) \times 10^{-11}$[b]
	233 – 348	$3.13 \times 10^{-12} \exp[(536 \pm 206)/T]$
Cronkhite *et al.* [24]	296	$(2.0 \pm 0.6) \times 10^{-11}$[a]
Bedjanian *et al.* [25]	298	$(3.1 \pm 0.8) \times 10^{-11}$
	230 – 360	$9.4 \times 10^{-12} \exp[(345 \pm 60)/T]$
Bloss *et al.* [26]	298	$(2.35 \pm 0.82) \times 10^{-11}$
IUPAC[37]	298	$(2.4 \pm 0.8) \times 10^{-11}$
	210 – 360	$4.5 \times 10^{-12} \exp[(500 \pm 200)/T]$
JPL NASA[2]	298	$(2.1 \pm 0.3) \times 10^{-11}$
		$4.5 \times 10^{-12} \exp(460/T)$

[a]*Under excess HO_2* [b]*Under excess BrO*

Table 2: Reaction scheme employed in the numerical model for BrO radical formation and subsequent decay.

Reaction	Rate coefficient[a] (760 Torr, function of T or at 298 K)
$Br + O_3 \rightarrow BrO + O_2$	$1.60 \times 10^{-11} \exp(-780/T)$
$Cl + O_3 \rightarrow ClO + O_2$	$2.30 \times 10^{-11} \exp(-200/T)$
$Cl + Cl (+ M) \rightarrow Cl_2 (+ M)$	$6.15 \times 10^{-34} \exp(906/T)$
$Br + Br \rightarrow Br_2$	$4.80 \times 10^{-15} \exp(1136/T)$
$Cl + Br_2 \rightarrow BrCl + Br$	$2.30 \times 10^{-10} \exp(-135/T)$[b]
$Br + Cl_2 \rightarrow BrCl + Cl$	1.70×10^{-15}[c]
$Cl + BrCl \rightarrow Cl_2 + Br$	1.45×10^{-11}[d]
$Br + BrCl \rightarrow Cl + Br_2$	3.30×10^{-15}
$Br + BrO \rightarrow Br_2O$	$1.90 \times 10^{-14} \exp(1370/T)$e
$Br_2O + Br \rightarrow BrO + Br_2$	4.00×10^{-11}[f]
$BrO + BrO \rightarrow Br + Br + O_2$	$1.92 \times 10^{-12} \exp(126/T)$[g]
$BrO + BrO \rightarrow Br_2 + O_2$	$3.40 \times 10^{-13} \exp(181/T)$[g]
	$2.50 \times 10^{-12} \exp(630/T)$[g]
$BrO + ClO \rightarrow Br + OClO$	$9.50 \times 10^{-13} \exp(550/T)$
$BrO + ClO \rightarrow Br + ClOO$	$2.30 \times 10^{-12} \exp(260/T)$
$BrO + ClO \rightarrow BrCl + O_2$	$4.50 \times 10^{-12} \exp(280/T)$[h]
$ClO + ClO (+ M) \rightarrow Cl_2O_2 (+ M)$	$k_0 = 1.60 \times 10^{-32} \times (T/300)^{-4.5}$[i]
$Cl_2O_2 \rightarrow ClO + ClO \rightarrow$	$k_\infty = 3.00 \times 10^{-12} \times (T/300)^{-2}$
	$K_{eq} = 1.72 \times 10^{-27} \exp(8649/T)$[j]
$Cl + O_2 \rightarrow ClOO$	$k_0 = 2.20 \times 10^{-33} \times (T/300)^{-3.1}$[i]
$ClOO \rightarrow Cl + O_2$	$k_\infty = 1.80 \times 10^{-10} \times (T/300)^{-0}$
	$K_{eq} = 6.60 \times 10^{-25} \exp(2502/T)$[j]

[a]Units are cm^3 $molecule^{-1}$ s^{-1} . All taken from NASA-JPL[2] unless otherwise stated, [b]taken from Bedjanian et al., [c]taken from Dolson et al., [d]taken from Baulch et al., [e]taken from Harwood et al., [f]taken from Rowley et al., [g]taken from Ferracci et al., [h]taken from Ferracci et al.,[24] [i]units of cm^6 $molecule^{-2}$ s^{-1} and [j]units of cm^3 $molecule^{-1}$

Table 3: Reaction scheme employed in the numerical model for HO_2 formation in the presence of BrO, and subsequent decay.

	Reaction	Rate coefficient[a] (760 Torr, function of T or at 298 K)
	$BrO + HO_2 \rightarrow HOBr + O_2$	$4.50 \times 10^{-12} \exp(460/T)$
	$Cl + CH_3OH \rightarrow CH_2OH + HCl$	5.50×10^{-11}
	$CH_2OH + O_2 \rightarrow HCHO + HO_2$	9.10×10^{-11}
	$Br + HO_2 \rightarrow HBr + O_2$	2.00×10^{-12}
	$HO_2 + HO_2 \rightarrow H_2O_2 + O_2$	$3.00 \times 10^{-13} \exp(460/T) + 5.17 \times 10^{-14} \exp(920/T)$ CH_3OH Enhancement: $k_{17f} \times (1 + (5.6 \times 10^{-22}) \times [CH_3OH] \times \exp((2550/T)))$
k_{18f}	$ClO + HO_2 \rightarrow HOCl + O_2$	$2.60 \times 10^{-12} \exp(290/T)$

[a]Units are cm^3 $molecule^{-1}$ s^{-1} unless otherwise stated [b]units of cm^6 $molecule^{-2}$ s^{-1} and [c]units of cm^3 $molecule^{-1}$

Table 4: Kinetic results from the BrO self-reaction (3)

T / K	$[Cl_2]_0/[Br_2]_0$	$[TR]_0$[a]/ 10^{14}	$k_{(3a)}$/ 10^{-12b}	$k_{(3b)}$/ 10^{-12b}	$k_{(3)}$/ 10^{-12b}
314.1	1.45 – 1.62	1.2 – 1.4	(2.78 ± 0.48)	(1.06 ± 0.12)	(3.84 ± 0.80)
298.15	1.05 – 2.29	1.5 – 1.9	(2.86 ± 0.10)	(1.32 ± 0.17)	(4.18 ± 0.56)
283	1.44 – 1.72	1.3 – 1.4	(3.12 ± 0.02)	(1.26 ± 0.06)	(4.38 ± 0.20)
268.15	1.32	(1.33 ± 0.07)	(3.02 ± 0.05)	(1.45 ± 0.21)	(4.47 ± 0.64)
257.15	1.85	(1.63 ± 0.04)	(2.65 ± 0.40)	(1.71 ± 0.04)	(5.20 ± 0.18)
246.15	1.44	(1.65 ± 0.04)	(3.49 ± 0.10)	(1.91 ± 0.33)	(4.56 ± 1.05)

[a]*Units in molecule* cm^{-3} [b]*Units in* cm^3 *molecule*$^{-1}$ s^{-1}

Table 5: Kinetic results from the BrO + HO_2 reaction (1)

T / K	$k_{(1)}$[a] / 10^{-11}	$[Cl_2]_0/[Br_2]_0$	$[CH_3OH]_0$[b] / 10^{17}
314.1	(2.55 ± 0.33)	1.45 – 1.62	1.75 – 4.38
298.15	(2.89 ± 0.31)	1.05 – 2.29	1.81 – 4.78
283.0	(3.08 ± 0.79)	1.44 – 1.72	0.97 – 3.86
268.15	(2.77 ± 0.52)	1.32	2.04 – 4.07
257.15	(2.73 ± 0.69)	1.85	1.06 – 1.60
246.15	(3.7 ± 1.5)	1.44	1.10

[a]*Units in cm^3 $molecule^{-1}$ s^{-1}* [b]*Units in molecule cm^{-3}*

Figures

Figure 1

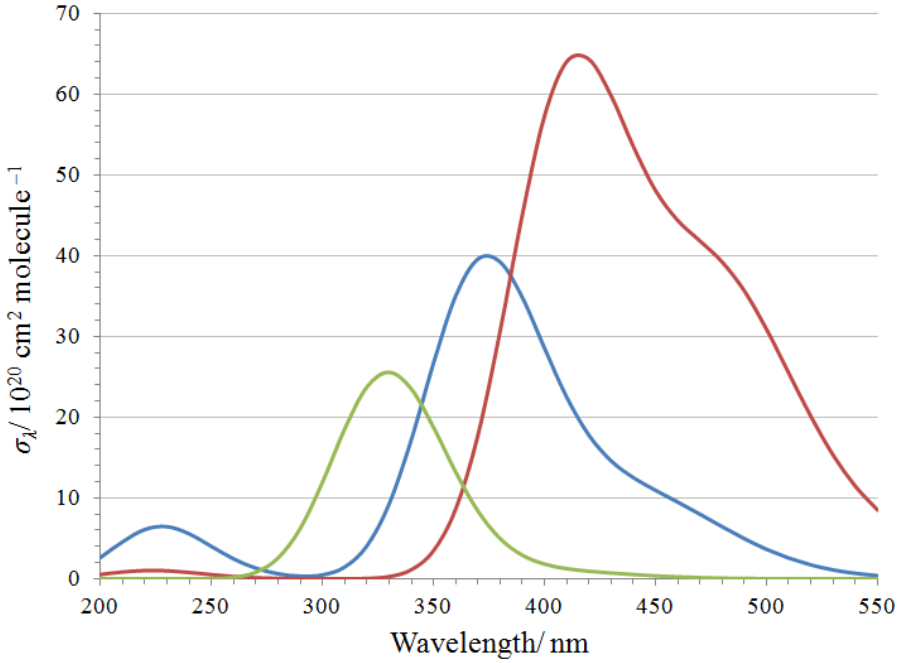

Figure 2

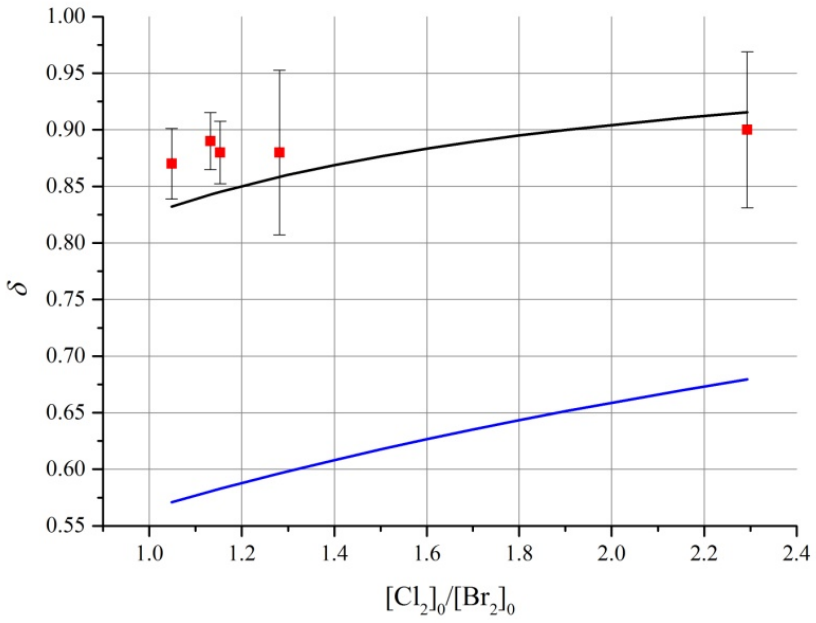
1.00
0.95
0.90
0.85
0.80
0.75
0.70
0.65
0.60
0.55
δ
1.0
1.2
1.4
1.6
1.8
2.0
2.2
2.4
[Cl2]0/[Br2]0

Figure 3

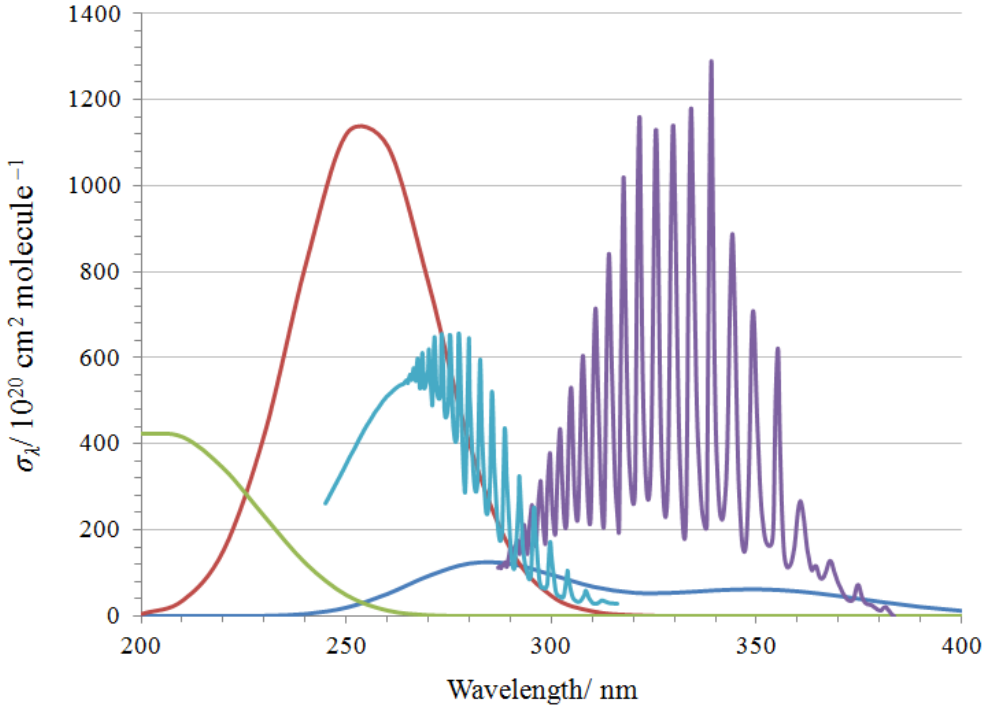
1400
1200
1000
800
600
400
200
0
200
250
300
350
400
σ_λ/ 10^{20} cm^2 molecule^{-1}
Wavelength/ nm

Figure 4

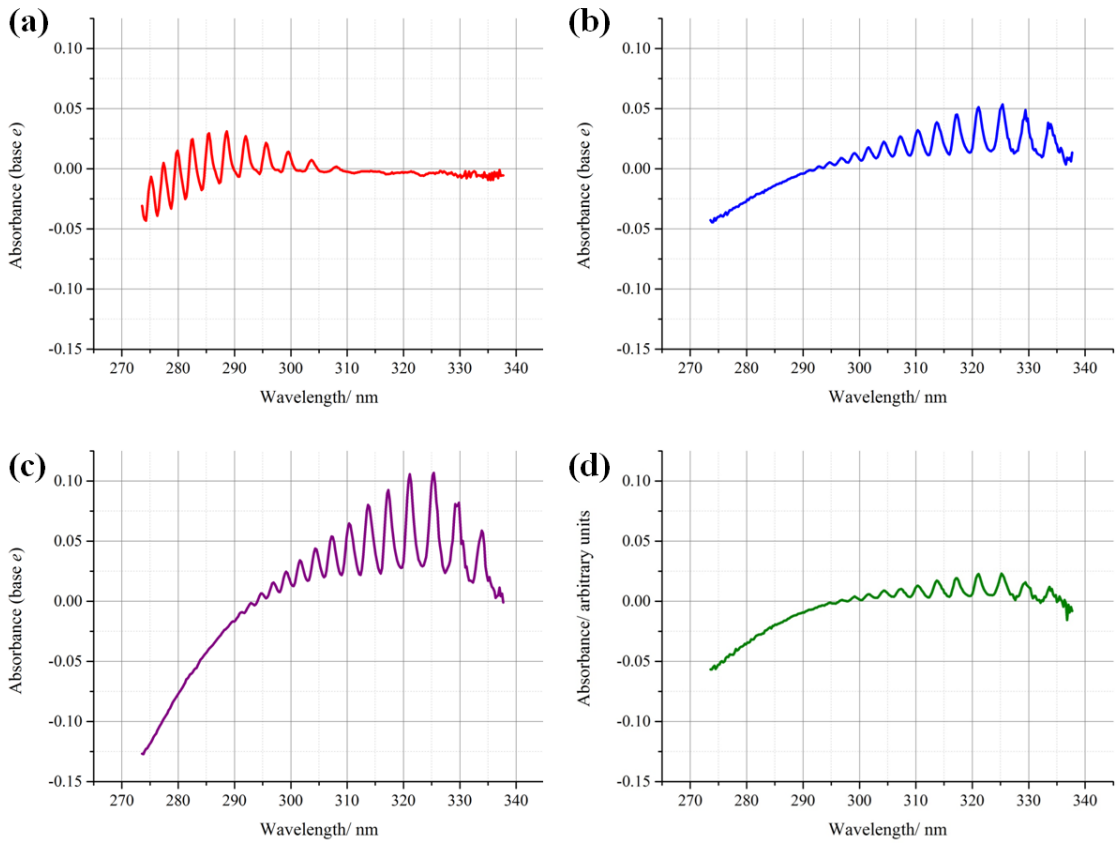
(a)
(b)
(c)
(d)
Absorbance (base e)
Absorbance/ arbitrary units
Wavelength/ nm
0.10
0.05
0.00
-0.05
-0.10
-0.15
270
280
290
300
310
320
330
340

Figure 5

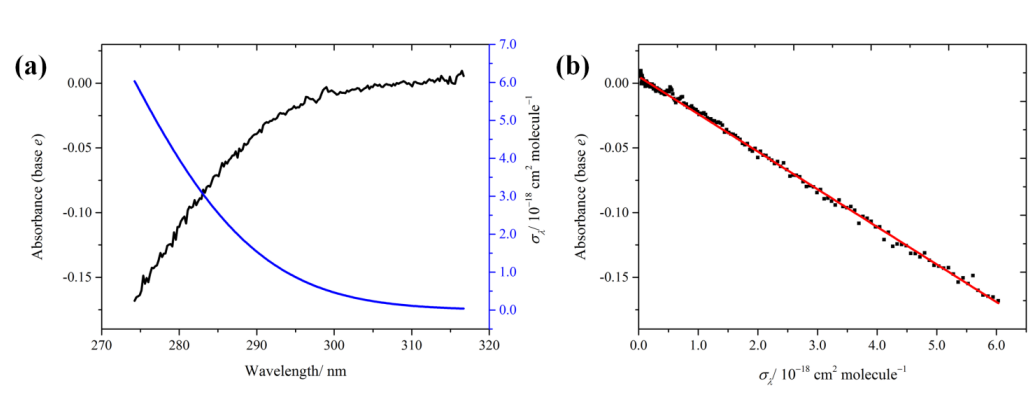
(a)
Absorbance (base e)
0.00
-0.05
-0.10
-0.15
270
280
290
300
310
320
Wavelength/ nm
7.0
6.0
5.0
4.0
3.0
2.0
1.0
0.0
σ_λ/ 10^{-18} cm^2 molecule^{-1}
(b)
Absorbance (base e)
0.00
-0.05
-0.10
-0.15
0.0
1.0
2.0
3.0
4.0
5.0
6.0
σ_λ/ 10^{-18} cm^2 molecule^{-1}

Figure 6

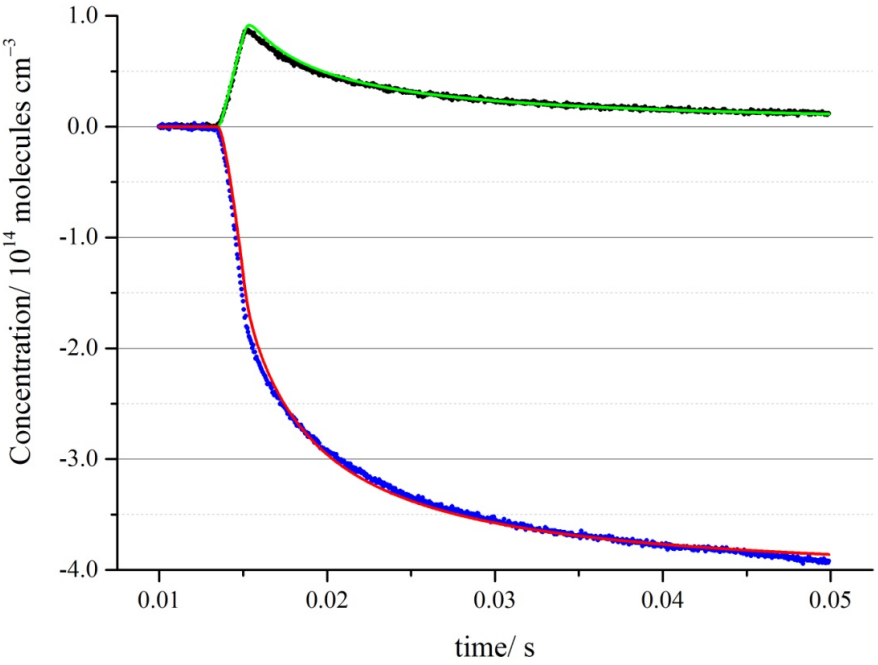
1.0
0.0
-1.0
-2.0
-3.0
-4.0
Concentration/ 10^14 molecules cm^-3
0.01
0.02
0.03
0.04
0.05
time/ s

Figure 7

(a)

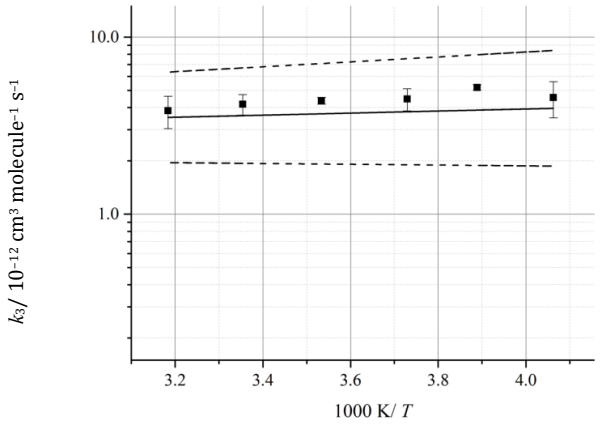
10.0
1.0
3.2
3.4
3.6
3.8
4.0
1000 K/ T
k3/ 10-12 cm3 molecule-1 s-1

(b)

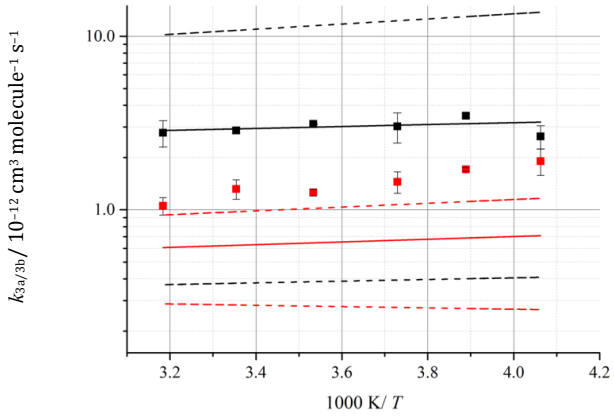
10.0
1.0
3.2
3.4
3.6
3.8
4.0
4.2
1000 K/ T
k3a/3b/ 10-12 cm3 molecule-1 s-1

Figure 8

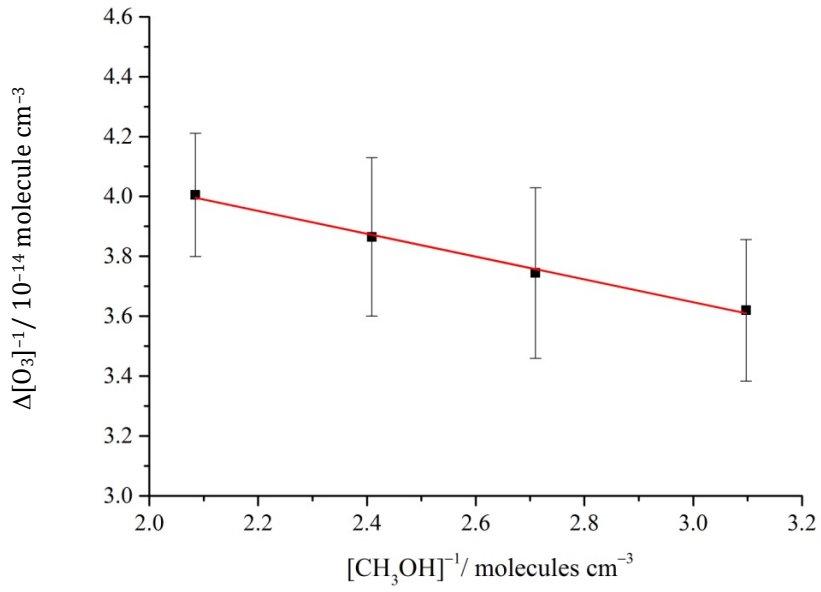
4.6
4.4
4.2
4.0
3.8
3.6
3.4
3.2
3.0
2.0
2.2
2.4
2.6
2.8
3.0
3.2
Δ[O3]-1 / 10-14 molecule cm-3
[CH3OH]-1 / molecules cm-3

Figure 9

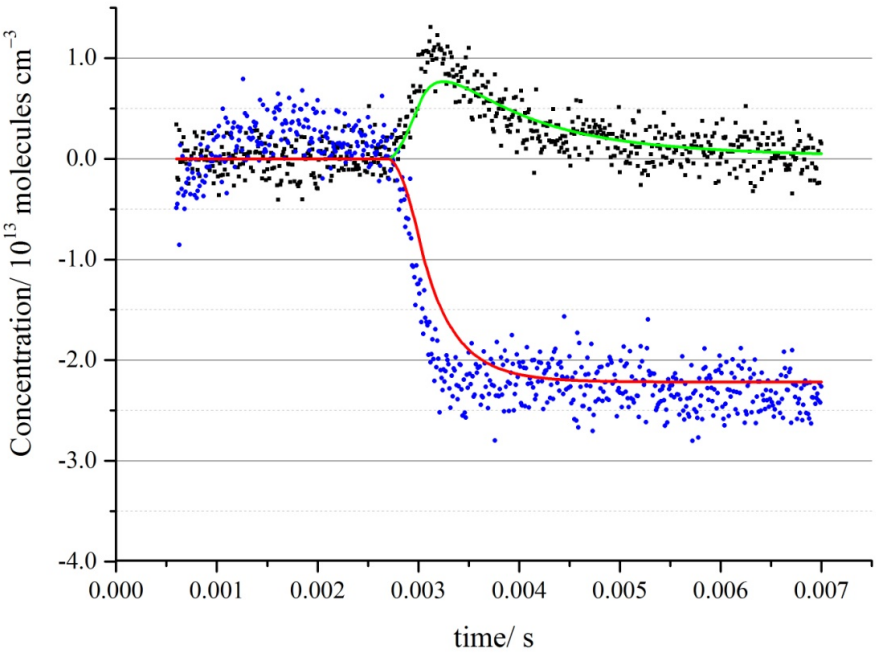
Concentration/ 10^13 molecules cm^-3
1.0
0.0
-1.0
-2.0
-3.0
-4.0
0.000
0.001
0.002
0.003
0.004
0.005
0.006
0.007
time/ s

Figure 10

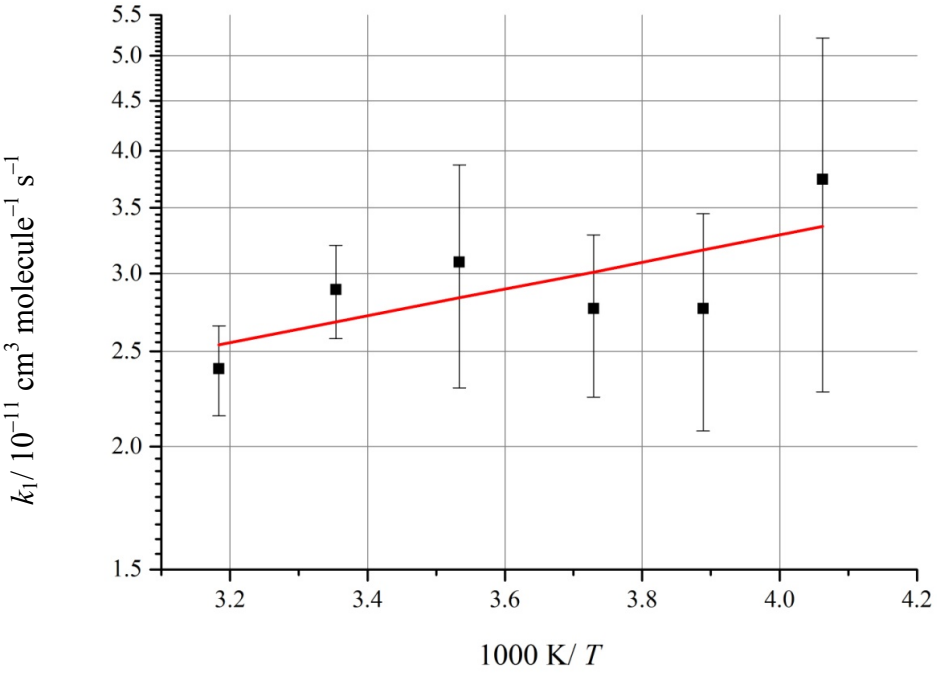
5.5
5.0
4.5
4.0
3.5
3.0
2.5
2.0
1.5
k_1/ 10^{-11} cm^3 molecule^{-1} s^{-1}
3.2
3.4
3.6
3.8
4.0
4.2
1000 K/ T

Figure 11

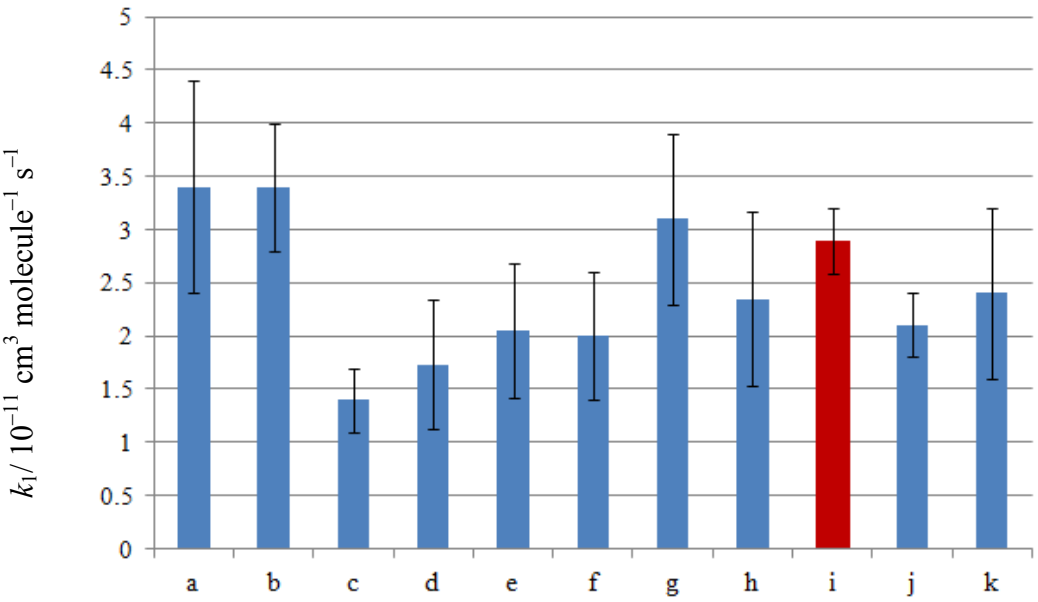

Figure 12

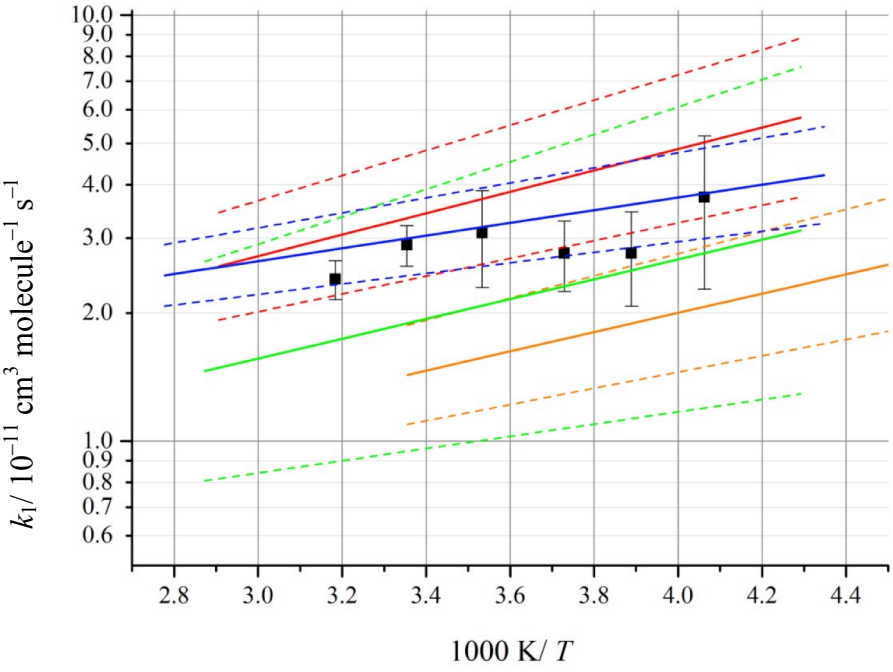
10.0
9.0
8.0
7.0
6.0
5.0
4.0
3.0
2.0
1.0
0.9
0.8
0.7
0.6
k_1/ 10^{-11} cm^3 molecule^{-1} s^{-1}
2.8
3.0
3.2
3.4
3.6
3.8
4.0
4.2
4.4
1000 K/ T

References

[1] W.R Simpson *et al. Chemical Reviews* 2015, **115** (10), 4035-4062, DOI 10.1021/cr5006638

[2] Sander, S.P., J. Abbatt, J. R. Barker, J. B. Burkholder, R. R. Friedl, D. M. Golden, R. E. Huie, C. E. Kolb, M. J. Kurylo, G. and G. K. Moortgat, *"Chemical Kinetics and Photochemical Data for Use in Atmospheric Studies, Evaluation No. 17,"* JPL Publication 10-6, Jet Propulsion Laboratory, Pasadena, 2011.

[3] M.K. Vollmer *et al.*, *J. Geophys Res. Atmospheres*, 2016, **121** (7), 3663-3686, 10.1002/2015JD024488.

[4] R.J. Salawitch, *"Atmospheric Chemistry - Biogenic Bromine". Nature*, 2006. **439**(7074): 275-277

[5] A. Saiz-Lopez, *et al.*, *Atmos. Chem. Phys.,* 2012, **12**, 3939–3949, DOI 10.5194/acp-12-3939-2012.

[6] *"Volcanism and Global Environmental Change"*, Ed. A. Schmidt *et al.*, 2015, Cambridge University Press.

[7] T.J. Roberts, R.S. Martin, L. Jourdain. 2014, **14** (20), 11201-11219. DOI: 10.5194/acp-14-11201-2014.

[8] P.J.Kelly *et al.*, *et al. Journal of Volcanology and Geothermal Research,* 2013, **259**. 317-333.

[9] J.H. Koo *et al.*, *Atmos. Chem. Phys.*, 2012, **12** (20), 9909-9922, DOI: 10.5194/acp-12-9909-2012.

[10] X. Yang *et al.*, *Atmos. Chem. Phys.*, 2010, **10** (16), 7763-7773, DOI: 10.5194/acp-10-7763-2010.

[11] K.A. Read *et al*., *Nature*, 2008, **453** (7199), 1232-1235. DOI: 10.1038/nature07035.

[12] S. Coburn *et al.*, *Atmos. Chem. Phys.*, 2016, **16** (6), 3743-3760, DOI: 10.5194/acp-10-7763-2010.

[13] B.M. Sinnhuber *et al.*, *Atmos. Chem. Phys.*, 2009, **9** (8), 2863-2871, DOI: 10.1002/2014GL062975

[14] J. Aschmann *et al.*, *Atmos. Chem. Phys.*, 2013, **13** (3), 1203-1219, DOI: 10.5194/acp-13-1203-2013.

[15] Yung, Y.L., J.P. Pinto, R.T. Watson, and S.P. Sander,. *Journal of the Atmospheric Sciences*, 1980. **37**(2), 339-353.

[16] Yang, X., *et al.*, *Journal of Geophysical Research-Atmospheres*, 2005. **110**(D23).

[17] R.J. Salawitch, *et al.*, *Geophys Res. Lett.* , 2005. **32**(5).

[18] Cox, R.A. and D.W. Sheppard, *Journal of the Chemical Society-Faraday Transactions Ii*, 1982. **78**: 1383-1389.

[19] Poulet, G., M. Pirre, F. Maguin, R. Ramaroson, and G. Lebras, *Geophysical Research Letters*, 1992. **19**(23): 2305-2308.

[20] Bridier, I., B. Veyret, and R. Lesclaux, *Chem. Phys. Lett.*, 1993. **201**(5-6): 563-568.

[21] Larichev, M., F. Maguin, G. Lebras, and G. Poulet,. *J. Phys. Chem.*, 1995. **99**(43): 15911-15918.

[22] Elrod, M.J., R.F. Meads, J.B. Lipson, J.V. Seeley, and M.J. Molina, *J. Phys. Chem.*, 1996. **100** (14): 5808-5812.

[23] Li, Z.J., R.R. Friedl, and S.P. Sander, *Journal of the Chemical Society-Faraday Transactions*, 1997. **93**(16): 2683-2691.

[24] Cronkhite, J.M., R.E. Stickel, J.M. Nicovich, and P.H. Wine,. *Journal of Physical Chemistry A*, 1998. **102**(33): 6651-6658

[25] Bedjanian, Y., V. Riffault, and G. Poulet,. *Journal of Physical Chemistry A*, 2001. **105**(13): 3167-3175.

[26] Bloss, W.J., D.M. Rowley, R.A. Cox, and R.L. Jones, *Phys. Chem. Chem.Phys.*, 2002. **4**(15): 3639-3647.

[27] Guha, S. and J.S. Francisco, *Journal of Physical Chemistry A*, 1999. **103**(40): 8000-8007.

[28] Kaltsoyannis, N. and D.M. Rowley, *Phys. Chem. Chem.Phys.*, 2002. **4**(3): 419-427.

[29] Ward, M. and D. M. Rowley, *Phys. Chem. Chem.Phys.*, 2016. 18(19): 13646-13656. DOI: 10.1039/c6cp00724d

[30] Ward, M. and D. M .Rowley, *Phys. Chem. Chem.Phys.*, 2016. 18(8): 6301-6315, DOI: 10.1039/c5cp07329d

[31] Stone, D. and D.M. Rowley, *Phys. Chem. Chem.Phys.*, 2005. **7**(10).

[32] Maric, D., J.P. Burrows, and G.K. Moortgat, *Journal of Photochemistry and Photobiology A: Chemistry*, 1994. **83**(3): 179-192.

[33] Ferracci, V. and D.M. Rowley,. *Phys. Chem. Chem.Phys.*, 2014. **16**(3): 1182-1196.

[34] Harwood, M.H., D.M. Rowley, R.A. Cox, and R.L. Jones, *J. Phys. Chem A*, 1998. **102**(10): 1790-1802.

[35] Rowley, D.M., M.H. Harwood, R.A. Freshwater, and R.L. Jones, *J. Phys. Chem*, 1996. **100**(8): 3020-3029.

[36] Wilmouth, D.M., T.F. Hanisco, N.M. Donahue, and J.G. Anderson,. *J. Phys. Chem A*, 1999. **103**(45): 8935-8945

[37] Baulch, D.L., J. Duxbury, S.J. Grant, and D.C. Montague, Evaluated Kinetic Data for High Temperature Reactions, Vol 4, - Homogeneous Gas-Phase Reactions of Halogen-Containing and Cyanide-Containing Species. *Journal of Physical and Chemical Reference Data*, 1981.
10: 1-721.